Table 2 Effect of α_1/α_2 on $\alpha_2 T_{cr}(Z = 26.6)$

	u_o restrained		u_o unrestrained	
α_1/α_2	$\alpha_2 T_{cr}$	n	$\alpha_2 T_{cr}$	n
0.3	110.0	44	119.6	47
	85.9[a]	36		
1.0	138.0	49	119.6	47
1.5	151.0	50	119.6	47

[a] Linear prebuckling analysis.

analysis. Also the shell deforms into smaller number of circumferential waves ($n = 36$). It can be seen from Table 2 that the parameter $\alpha_2 T_{cr}$ increases in magnitude for increasing values of α_1/α_2 ratio.

Effect of boundary conditions on $\alpha_2 T_{cr}$

The critical parameter $\alpha_2 T_{cr}$ for a shell with $Z = 1.89$, for all the boundary conditions c-1 to c-4 are given in Table 3. It can

Table 3 Effect of different buckling conditions on $\alpha_2 T_{cr}(Z = 1.89)$

Boundary conditions	$\alpha_2 T_{cr}$	n
c-1	80.87	54
c-2	80.20	50
c-3	80.70	54
c-4	78.10	49

be seen that the critical temperature of a cylinder, constrained axially is unaffected whether the circumferential edge is restrained or free. If the axial displacement is released, the buckling parameter is lower when the displacement v_n is unrestrained than when restrained. However the difference is not considerable. Irrespective of the boundary conditions used in the circumferential direction, the number of circumferential waves for axially restrained cylinder is more than the unrestrained case.

Conclusions

The results for clamped cylinders indicate that for lower values of geometric parameter ($Z \leqq 3.7$) the symmetric mode of buckling is predominant while for $Z \leqq 3.7$, the asymmetric mode governs the behavior. Inclusion of prebuckling rotations in the analysis estimates higher buckling temperature. The critical temperature is higher for increasing values of the α_1/α_2 ratio. The buckling boundary conditions do not significantly alter the buckling behavior.

References

[1] Hoff, N. J., "Buckling of Thin Cylindrical Shell under Hoop Stress Varying in Axial Direction," *Journal of Applied Mechanics*, Vol. 24, 1957, pp. 405–412.

[2] Johns, D. J., "Local Buckling of Thin Circular Cylindrical Shells," *Collected Papers on Instability of Shell Structures*, TN-D 1510, Dec. 1962, pp. 266–276, NASA.

[3] Anderson, M. S., "Thermal Buckling of Cylinders," Collected Papers on Instability of Shell Structures, TN-D 1510, Dec. 1962, pp. 255–265, NASA.

[4] Bushnell, D., "Analysis of Ring Stiffened Shells of Revolution Under Combined Thermal and Mechanical Loading," *AIAA Journal*, Vol. 9, No. 3, March 1971, pp. 401–410.

[5] Chang, L. K. and Card, M. F., "Thermal Buckling Analysis for Stiffened Orthotropic Cylindrical Shells," TN-D 6332, April 1971, NASA.

[6] Bushnell, D., "Non-Symmetric Buckling of Cylinders with Axisymmetric Thermal Discontinuities," *AIAA Journal*, Vol. 11, No. 9, Sept. 1973, pp. 1292–1295.

[7] Bushnell, D. and Smith, S., "Stress and Buckling of Nonuniformly Heated Cylindrical and Conical Shells," *AIAA Journal*, Vol. 9, No. 12, Dec, 1971, pp. 2314–2321.

[8] Dasgupta, S. and Wang I-Chih, "Thermal Buckling of Orthotropic Cylindrical Shells," *Fibre Science and Technology*, Vol. 6, No. 1, Jan. 1973, pp. 39–45.

[9] Radhamohan, S. K. and Prasad, B., "Asymmetric Buckling of Toroidal Shells under Axial Tension," *AIAA Journal*, Vol. 12, No. 4, April 1974, pp. 511–515.

[10] Radhamohan, S. K., Setlur, A. V., and Goldberg, J. E., "Stability of Shells by Parametric Differentiation Technique," *Journal of Structural Division, Proceedings of the ASCE*, Vol. 97, June 1971, pp. 1775–1790.

Prevention of Delamination of Composite Laminates

N. J. PAGANO*
Air Force Materials Laboratory, Dayton, Ohio
AND
L. M. LACKMAN†
Rockwell International, Los Angeles, Calif.

As described by Dickerson and Lackman,[1] the longerons of the B-1 air vehicle consist of a basic metal element with an adhesively bonded boron/epoxy cross-ply laminate. Concern with regard to free edge delamination caused by interlaminar normal stress σ_z[2-4] has led to a design in which the 90° layers have been "softened" in the vicinity of the free edges by means of a mechanical serrating process as shown in Fig. 1. In this Note, we shall present some experimental observations with respect to the effectiveness of this procedure for large diameter boron/epoxy laminates under static and fatigue (tension) loadings. Specifically, we shall consider the extreme case of a laminate that is highly prone toward delamination and observe the influence of serration on its delamination threshold, ultimate strength, and fatigue life.

It should be noted that one approach to prohibit delamination has already been proposed in the literature.[2] This involves the prescription of a detailed stacking sequence such that inter-

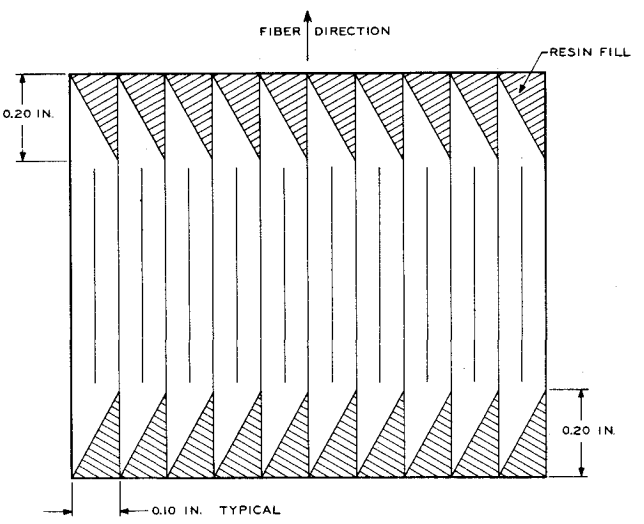

Fig. 1 Serration pattern.

Presented as Paper 74-355 at the AIAA/ASME/SAE 15th Structures, Structural Dynamics and Materials Conference, Las Vegas, Nev., April 17–19, 1974; submitted May 1, 1974; revision received September 3, 1974.

Index category: Structural Composite Materials (including Coatings).

* Materials Research Engineer, Nonmetallic Materials Division.

† Manager, Composite Programs, Los Angeles Aircraft Division.

laminar *compression* is induced in the neighborhood of a free edge. While this approach is sound, it fails as a universal remedy in structural elements that are subjected to extreme reversals in direction of applied loading. This concept, however, may be employed to experimentally determine the *laminate ultimate strength,* which is defined as the stress level at which a laminate specimen suffers complete fracture in the absence of delamination.

Following the procedure developed by Pagano and Pipes,[3] we can design a laminate which is subjected to high tensile values of σ_z within the free edge zone for the particular material under study (boron/epoxy). This specimen

T: (30°, −30°, 30°, −30°, 90°, 90°, 90°, −30°, 30°, −30°, 30°)

serves as our delamination sample. If we revise the stacking sequence as follows,

C: (90°, 30°, −30°, 30°, −30°, 90°, −30°, 30°, −30°, 30°, 90°)

we find that σ_z is *compressive* adjacent to the free edges, so that this laminate is not susceptible to delamination. Hence, the latter will be used to define the laminate ultimate strength. Finally, the symbol TS will be used to represent laminates in which the layers are arranged in accordance with T, but in which the 90° are serrated as shown in Fig. 1 and resin is substituted for the material removed. Constant amplitude fatigue tests at a stress ratio $R = 0.1$ were conducted in addition to static tension experiments.

The results of the static tension tests are displayed in Table 1,

Table 1 Experimental data (static tension)

Laminate	T	T	TS	TS	C	C
E_L, 10^6 psi	11.2	12.2	10.9	11.0	12.2	12.3
σ_u, 10^3 psi	*a*	72	95	93	97	102
ε_u, 10^{-3} in./in.	*a*	10.7	9.8	10.7	9.5	9.6
σ_D, 10^3 psi	34	37	...	...	...	...
ε_D, 10^{-3} in./in.	3.1	3.1	...	...	...	...

[a] Specimen was not tested to failure (saved for demonstration purposes).

where σ and ε refer to applied axial stress and strain, respectively. The stresses σ_D and σ_u are those acting at the onset of delamination and at ultimate failure, respectively, while ε_D and ε_u are the corresponding axial strains. As only a few samples of each configuration were tested, the observed data for each sample are indicated in the table. Specimens TS and C exhibited no visible delamination under static loading and we notice that the ultimate strength of TS is comparable to the respective strength of C, which is defined as the laminate ultimate strength. Conversely, in the T laminate, the delamination threshold occurs at approximately one-third of laminate ultimate strength, the delamination crack extending along the entire length of the coupon as shown in Fig. 2, which leads to the apparent loss in ultimate strength indicated in Table 1. While the latter observation is based upon only one data point, a comparable loss in residual strength after a small number of fatigue cycles lends credibility to this type of behavior. It should be noted that an analogous strength degradation was not observed in graphite/epoxy composites.[3]

Laminate T may be used as the basis for characterizing the delamination strength of the present material provided one can estimate the initial curing stresses induced in fabrication processing. For this purpose, we assume an elastic stress field resulting from a 200°F temperature drop, in conjunction with the room temperature material properties cited by Dickerson and Lackman.[1] By the method given in Ref. 4, we calculate the maximum value of interlaminar normal stress at the onset of delamination to be 18.6 ksi. It should be noted, however, that effective modulus stress analyses, as employed here, lose their meaning in the presence of severe macroscopic stress gradients, with the possible exception of characterizing average values of stress over representative volume elements. This point, which is

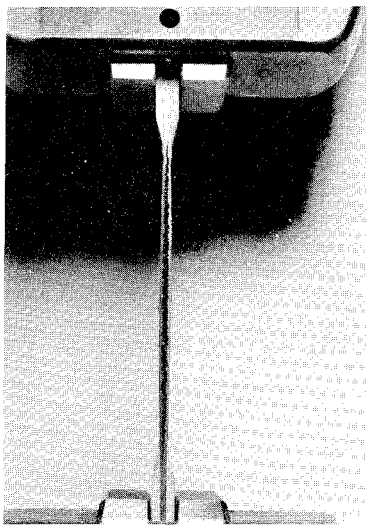

Fig. 2 Delamination specimen.

more fully discussed by Pagano and Rybicki,[5] is of particular significance in relation to composites made with large fibers, such as the present ones. We therefore determine the average value of σ_z over a length of one fiber spacing (0.007″) adjacent to the free edge at the onset of delamination. This value, $\bar{\sigma}_z = 12$ ksi, is comparable to the transverse tensile strength of boron/epoxy. In these calculations, we have replaced the contiguous $\pm 30°$ layers by a homogeneous material possessing the same effective extensional stiffness matrix and thermal expansion coefficients as a symmetric $\pm 30°$ angle-ply.[6]

The fatigue behavior of the T-laminate, at least when the maximum applied stress σ_F is lower than σ_D, is characterized by early delamination and fairly long lifetimes. For example at 30 ksi, $R = 0.1$, one specimen delaminated at 1200 cycles and completely ruptured at 2.8×10^6 cycles. Another also suffered early delamination prior to 58,000 cycles, the precise initiation of delamination being missed, and complete rupture at 1.4×10^6 cycles. A third specimen was tested at 27 ksi, $R = 0.1$ until delamination occurred at 4100 cycles at which point it was subjected to a residual static tensile strength test. As noted earlier, a severe strength reduction ($\sigma_u = 66$ ksi) was observed. In the latter test, E_L was degraded to 7.8×10^6 psi, while the failure strain had the value 0.0107. In conducting these as well as subsequent fatigue tests, the frequency was generally held at 1 cps prior to delamination and subsequently raised to 5 cps.

Fatigue tests conducted on TS specimens seem to define two distinct types of response. For the case $\sigma_F < \sigma_{CR}$, where σ_{CR} is a critical stress somewhere in the range of 30–40 ksi, the specimen behavior is characterized by the absence of delamination and long lifetimes. For $\sigma_F > \sigma_{CR}$, incipient delamination is followed quickly by catastrophic rupture, the response being characterized by fairly short lifetime. The fatigue data for the TS specimens is given in Table 2, where the symbol N stands for number of cycles. The runout specimen was subjected to a residual strength test with the following results: $E_L = 9.5 \times 10^6$ psi, $\sigma_u = 86$ ksi, $\varepsilon_u = 0.0094$.

Table 2 TS Tensile fatigue data, $R = 0.1$

σ_F (ksi)	N_D	N_u
30	...	5.4×10^6
30	...	1.03×10^6
		Runout
40	103×10^3	131×10^3
40	*a*	118×10^3
50	*a*	4.5×10^3
50	*a*	6.3×10^3
50	58.8×10^3	59×10^3

[a] *Failed specimens exhibit delaminations, but incipient point was missed.*

In conclusion, for the extreme case of delamination-prone laminates characterized here, the serration procedure of Ref. 1 has been shown to be effective in withstanding free edge delamination under static loading and resisting applied stresses comparable to laminate ultimate strength. Under sufficiently high stress levels in a fatigue environment, however, a highly undesirable (catastrophic) failure mode occurs. This indicates that tensile values of σ_z are present at the free edge in TS, however, at lower stress concentration than in T. Subsequent to precipitation of delamination under fatigue loading, stress concentrations at the internal corners of the serrations evidently dominate the fracture response. Conceivably, alteration of the serration geometry, in particular, elimination of the sharp corners, may lead to improved failure characteristics.

References

[1] Dickerson, E. O. and Lackman, L. M., "Boron-Reinforced Longerons," *Proceedings of the Conference on Fibrous Composites in Flight Vehicle Design*, AFFDL-TR-72-130, Air Force Flight Dynamics Laboratory, Wright-Patterson Air Force Base, Ohio, pp. 583–617.

[2] Pagano, N. J. and Pipes, R. B., "The Influence of Stacking Sequence on Laminate Strength," *Journal of Composite Materials*, Vol. 5, Jan. 1971, pp. 50–57.

[3] Pagano, N. J. and Pipes, R. B., "Some Observations on the Interlaminar Strength of Composite Laminates," *International Journal of Mechanical Sciences*, Vol. 15, 1973, pp. 679–688.

[4] Pagano, N. J., "On the Calculation of Interlaminar Normal Stress in Composite Laminates," *Journal of Composite Materials*, Vol. 8, Jan. 1974, pp. 89–105.

[5] Pagano, N. J. and Rybicki, E. F., "On the Significance of Effective Modulus Solutions for Fibrous Composites," *Journal of Composite Materials*, Vol. 8, July 1974, pp. 214–228.

[6] Pagano, N. J., "Exact Moduli of Anisotropic Laminates," in *Mechanics of Composite Materials*, Vol. 2, edited by G. P. Sendeckyj, Academic Press, New York, 1974, pp. 23–44.

Vibrations of Sandwich Beams with Central Masses

SHAUKAT MIRZA* AND ANAND V. SINGH†

University of Ottawa, Ottawa, Canada

Introduction

SEVERAL papers dealing with the vibration of beams having masses have been published in the past.[1-3] With the increasing use of sandwich construction in the modern technology, efforts have also been made in studying the dynamic response of layered beams, plates, and shells without any mass.[4-6]

In this Note an attempt has been made to study the natural frequencies of vibration of sandwich beams with central masses. A treatment of this type of problem is not available in the literature. The beam considered in this study is composed of isotropic thin face sheets and a thick core. The two face sheets are considered to be thin and of equal thickness h. The thickness of the core is taken as c (Fig. 1). Because of the presence of mass M, two separate cases for symmetric and antisymmetric modes have been investigated.

Basic Equations

While arriving at the differential equations, the following assumptions have been used: 1) The face sheets are completely bonded to the core and there is no slip at the interfaces; 2) The core takes bending stresses in the plane of the sandwich; 3) The thin face sheets behave as membranes; 4) The extensional rigidity of the core in the lateral direction is infinite.

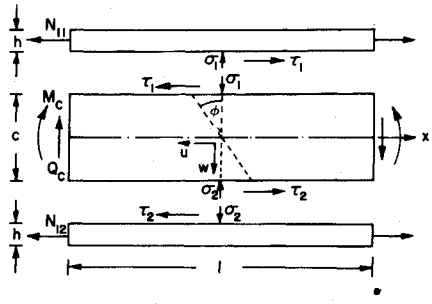

Fig. 1 Sandwich beam element showing displacements, stresses at the interfaces and on the cross-section.

The last assumption leads to the incompressibility condition of the core. The following relation is then easily established: $w_c = w_1 = w_2 = w$. The quantity w denotes the lateral deflection and the subscripts c, 1 and 2 refer to the core, the first and second face sheets, respectively. In writing the differential equations of motion, the rotary inertia of the face sheets and the core about the middle plane is neglected. This is a valid assumption, as we are concerned with the frequencies which are much below the first thickness shear frequency of the sandwich beam.

Writing the equations of motion for the core, the first and second face sheets, and eliminating the unknown interface stresses σ_1, σ_2, τ_1, and τ_2 by combining these equations, yields the following two equations,[4]

$$\begin{aligned} B\,\partial^2\phi/\partial x^2 - G_c A_c(\phi + \partial w/\partial x) &= 0 \\ G_c A_c(\partial\phi/\partial x + \partial^2 w/\partial x^2) &= m\,\partial^2 w/\partial t^2 \end{aligned} \tag{1}$$

The rotation of the transverse plane of the core and its cross sectional area are given by ϕ and A_c, respectively. Further, the shear modulus and the density of the materials of the core are represented by G_c and ρ_c. Since the present investigation deals with the free vibrations, Eqs. (1) do not contain the external loading terms. For convenience the following symbols have been introduced in Eqs. (1) and elsewhere in this Note

$$B = \tfrac{1}{2}EA_f c^2 + E_c I_c$$
$$m = \rho_c A_c[1 + 2\rho h/(\rho_c c)]; \quad K = G_c A_c$$

The modulus of elasticity and the density of the face sheets are given by E and ρ. The quantity A_f represents the cross-sectional area of a face sheet. The governing differential equation can be obtained by combining Eqs. (1) which yields the equation in terms of deflection w.

$$\partial^4 w/\partial x^4 - (m/K)\,\partial^4 w/\partial x^2\,\partial t^2 + (m/B)\,\partial^2 w/\partial t^2 = 0 \tag{2}$$

Symmetric and Antisymmetric Modes

The mass M which has a moment of inertia I^* is placed at the mid-span of the beam. The first part of the Note deals with the analysis of the symmetric modes and the later section with asymmetric modes. Two cases of simple-simple and fixed-fixed support conditions have been considered in each of these two sections. Because of the presence of the mass M, it is necessary to write these conditions separately for symmetric and nonsymmetric modes.

The normal mode solution of Eq. (2) in terms of the two variables w and ϕ is given in the form,

$$\begin{aligned} w(x,t) &= \sum W_n(x)\sin(\Omega_n t) \\ \phi(x,t) &= \sum \Phi_n(x)\sin(\Omega_n t) \end{aligned} \tag{3}$$

This separation of variables technique yields a pair of ordinary differential equations. The differential equations in the spatial variable are then solved. The solution is of the form

Received July 1, 1974; revision received August 26, 1974.

Index categories: Structural Dynamic Analysis; Aircraft Vibration.

* Associate Professor, Department of Mechanical Engineering.

† Research Assistant, Department of Mechanical Engineering.